RSC Advances

PAPER

View Article Online
View Journal | View Issue

Cite this: *RSC Adv.*, 2020, **10**, 28300

The interaction between oxytocin and heparin

Einat Schnur* and Timothy R. Rudd*

Oxytocin (**OXT**) is a small cyclic peptide that is administered to pregnant women to induce birth in cases where labour is prolonged. It has previously been observed that patients taking a low molecular weight heparin, dalteparin (**DAL**), and then prescribed, **OXT** experienced a swifter labour compared to women given **OXT** alone. Herein are described the interactions between **OXT** and a number of heparin-based oligosaccharides; **DAL**; fondaparinux (**FP**), which is a synthetic heparin oligosaccharide that represents the predominant antithrombin binding-site, and a family of chemically-derived heparin hexasaccharides. The latter oligosaccharides were chosen as they represent sequences found within the polysaccharide dalteparin. Furthermore, the carbohydrate chemical space was investigated by comparing the interaction between **OXT** and four chemically derivatived heparin hexasaccharides; I_{2S}-A^{6S}_{NS} (**DP6**), I_{2OH}-A^{6S}_{NS} (**DP6-2OH**, de-2-*O*-sulfated hexasaccharide), I_{2S}-A^{6OH}_{NS} (**DP6-6OH**, de-6-*O*-sulfated hexasaccharide) and I_{2S}-A^{6S}_{NAc} (**DP6-NAc**, de-*N*-sulfated hexasaccharide). The interactions between the peptide and oligosaccharides were studied using a series of ^{13}C–^{1}H and ^{15}N–^{1}H HSQC NMR experiments, at a range of temperatures. This approach allowed the binding epitopes of the peptide and oligosaccharides to be identified, highlighting that 6-*O*- and *N*-sulfation substituent groups of heparin are important for the interaction between the peptide and carbohydrate. This is an important observation as de-*N*-sulfation is a traditional method for decreasing the anticoagulation properties of heparin. Furthermore, low temperature experiments of the **OXT** : **FP** complex indicate that hydrogen-bonding is very important for the interaction between the peptide and oligosaccharide.

Received 11th May 2020
Accepted 20th July 2020

DOI: 10.1039/d0ra04204h

rsc.li/rsc-advances

1. Introduction

Heparin has been used as an anticoagulant in the clinic for over 80 years,[1] the anticoagulant activity is driven through interactions with members of the clotting cascade, most notably thrombin and antithrombin.[2] Heparin is a biological medicine, being derived from living organisms, the majority of which is extracted from the intestinal mucosa of pigs.[3]

Heparin is a linear polyanionic carbohydrate, composed of the repeating disaccharide unit of an uronic acid bound to glucosamine through (1 → 4) glycosidic linkages. Heparin is heterogenous due to the carbohydrate's variable chain lengths and different substitutions of the disaccharide subunits. The uronic acid residue is primarily α-L-iduronic acid but is also present as its C-5 epimer β-D-glucuronic acid. Also, the uronic acid can be *O*-sulfated at position-2. The *N*-glucosamine can be decorated by sulfates at several positions. At position-2 (the amino function) the glucosamine can carry either an acetyl, sulfate or amine group. Furthermore, the glucosamine can be *O*-sulfated at position-6 and more rarely at position-3 (Fig. 1A).[4] The primary, but not exclusive, binding site of antithrombin in heparin is a pentasaccharide containing an α-D-glucosamine that is trisulfated; *O*-sulfated at positions-3 and -6 and *N*-sulfated. The sequence of the pentasaccharide can be found in Fig. 1C.[5]

Low molecular weight heparins (LMWH) are heparins that have been depolymerised using chemical or enzymatic means to give rise to this class of compounds with a molecular weight of less than 8000 Da.[6] They are enriched in the antithrombin binding domain (which is a consequence of the resistance of this trisulfated residue to the chemical process used) and have improved pharmaco-kinetics/-dynamics compared to unfractionated heparin. An important property of LMWHs is that they induce fewer incidences of thrombocytopenia, which is an immune response to the complex between platelet factor 4 and heparin.[7]

Oxytocin (**OXT**) is a nonapeptide hormone of the following sequence; Cys–Tyr–Ile–Gln–Asn–Cys–Pro–Leu–Gly (Fig. 1E). It forms a cyclic structure, maintained by a disulfide bond between the two cysteine residues and its C-terminus is converted to an amide. Oxytocin can be found in multiple locations in the body and has been implicated in a wealth of physiological and psychological conditions.[8] It is best known for its role in uterine muscles contractility, which was first demonstrated in cats,[9] and is being administered as a drug to initiate and accelerate labour.[10] The biological activity of **OXT** is mediated through oxytocin receptors, these are G-protein-coupled receptors that also require magnesium[11] and cholesterol.[12]

National Institute of Biological Standards and Control, Blanche Lane, South Mimms, Potters Bar, Hertfordshire, EN6 3QG, UK. E-mail: einat.schnur@nibsc.org; tim.rudd@nibsc.org

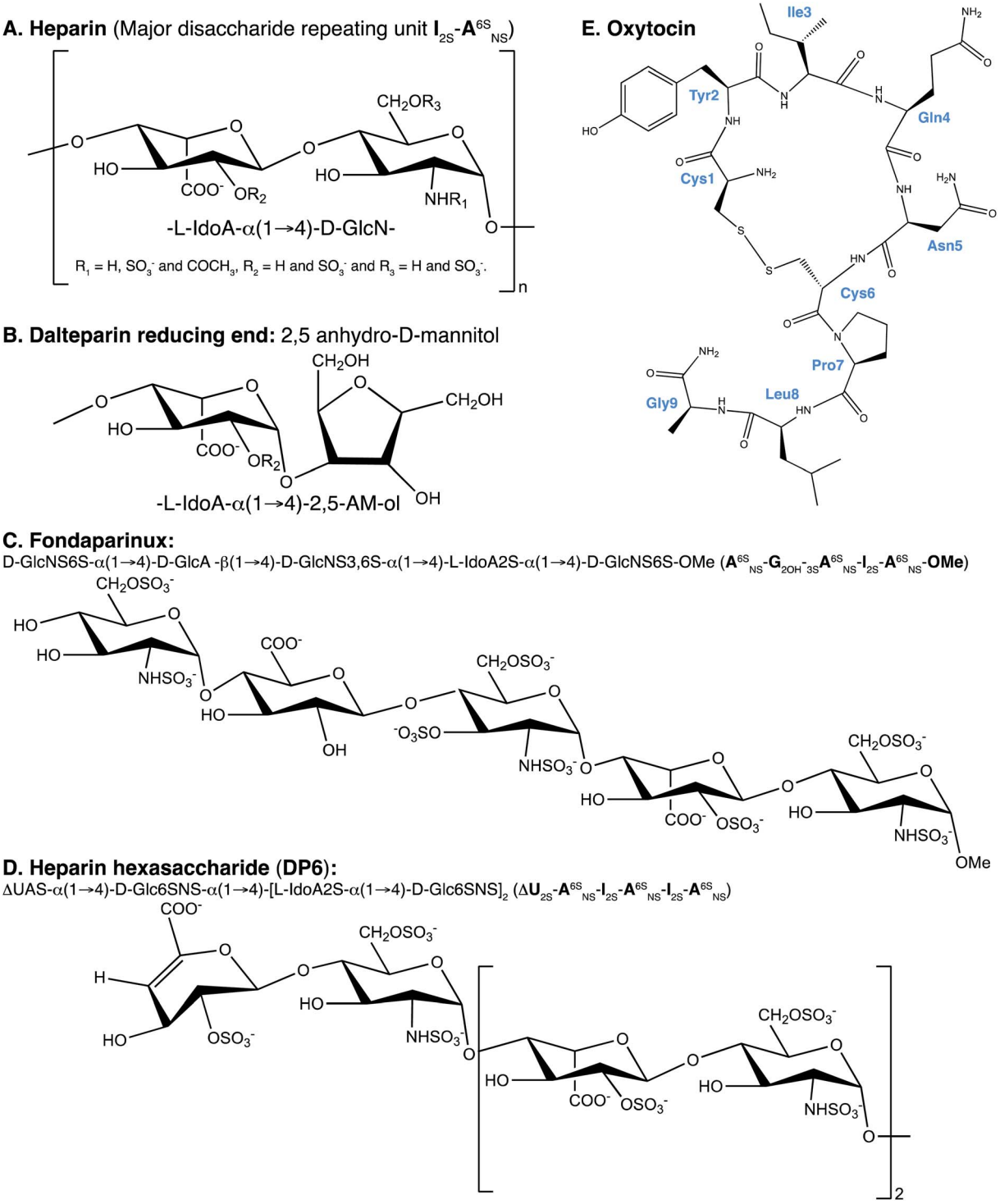

Fig. 1 Illustration of the structures of (A) heparin, the major repeating unit of which is the trisulfated disaccharide I_{2S}-$A^{6S}{}_{NS}$; (B) the nominal reducing end of DAL, an iduronic acid group linked to 2,5 anhydrous-D-mannitol (2,5-AM-ol), the terminal group can also be sulfated at position 6 (6-*O*-sulfo-2,5-anhydro-D-mannitol); (C) fondaparinux (FP), (D) the trisulfated heparin hexasaccharide DP6 and (E) OXT, where the amino acids are labelled in blue. I stands for iduronate, G for glucuronic acid, A for glucosamine, ΔU for an unsaturated uronic acid and nr indicates that the residue is at the nonreducing end of the molecule. The sub- and superscripts denote the position of sulfation (S) or acetylation (NAc), respectively. AN and IN refer to position N (either C atom or H atom depending on the context) of the glucosamine or iduronate residue, respectively. For example, I_{2S}-$A^{6S}{}_{NS}$ corresponds to the disaccharide 2-O sulfated iduronic acid linked to 6-*O*-sulfated *N*-sulfated glucosamine. A2* signifies position 2 of glucosamine, which is *N*-sulfated and *O*-sulfated at positions 6 and 3.

Recently, it has been shown that when low molecular weight heparin, dalteparin (**DAL**), is administered to pregnant women in combination with **OXT**, the patients exhibited greatly reduced labour times, compared to administration of **OXT** alone.[13] The mechanism for this is two-fold; firstly low molecular weight heparin effects cervical ripening. Secondly, there are indications that heparin interacts with the oxytocin signalling pathway alone.[13] This effect is also discussed in the review by Lindahl *et al.*,[14] interestingly this review is centred on the fact that heparan sulfate has been implicated in many disease, but the use of heparin/heparan sulfate-based drugs is still underutilised. Dalteparin is produced from heparin that is extracted from porcine intestinal mucosa. The unfractionated heparin undergoes deaminative cleavage with nitrous acid, followed by reduction and a chromatographic purification process.[15] The depolymerisation process results in the formation of a 2,5-anhydro-D-mannitol ring at the reducing end of the polysaccharide, which can be used to identify the LMWH[16] (Fig. 1B). The main drawback in using **DAL** as a birthing aid is that the LMWH is an anticoagulant. To this end, a non-anticoagulant LWMH is being developed by Dilafor AB and Opocrin S.p.A, tafoxiparin. This product is currently undergoing trials, entitled 'Effect of Tafoxiparin on Cervical Ripening and Induction of Labour in Term Pregnant Women With an Unripe Cervix' and has been assigned the following identifier, NCT04000438.[17]

The work presented herein investigates a direct interaction between **OXT** and heparin oligosaccharides, using nuclear magnetic resonance (NMR) spectroscopy. With the aim of identifying the site of interaction in both molecules. Initially, three oligosaccharides were used; **DAL**, the low molecular weight heparin first observed to have a synergistic affect with **OXT**, fondaparinux (**FP**) and a heparin hexasaccharide (**DP6**). Fondaparinux is a pentasaccharide produced synthetically (Fig. 1C), which here, serves as a model compound for the heparin antithrombin binding site.[18–20] The heparin hexasaccharide **DP6** has an average composition of three disaccharide repeating units of 2-*O*-sulfated iduronic acid linked to 6-*O*- and 2-*N*-sulfated glucosamine [$\mathbf{I}_{2S}$-$\mathbf{A}^{6S}{}_{NS}$]$_3$ (Fig. 1D). It represents the general sequence of heparin. Dalteparin is a heterogenous mixture of large molecules not ideal for NMR studies and, since **DAL** is comprised of regions containing both **FP** and **DP6**, it was logical to investigate the interaction of **OXT** with **FP** and **DP6**, as well as with **DAL**.

The study between **OXT** and heparin was then directed towards investigating the diverse chemical space of heparin and the affect the different sequences found within heparin has on the interaction with **OXT**. A panel of four heparin hexasaccharides were chosen, with three of the hexasaccharides containing specific chemical modifications; de-2-*O*-sulfated iduronic acid ([$\mathbf{I}_{2OH}$-$\mathbf{A6S}_{NS}$]$_3$), de-6-*O*-sulfated glucosamine ([$\mathbf{I}_{2S}$-$\mathbf{A}^{6OH}{}_{NS}$]$_3$) and *N*-acetylated glucosamine ([$\mathbf{I}_{2S}$-$\mathbf{A}^{6S}{}_{NAc}$]$_3$). The fourth member of the panel is the orthodox trisulfated heparin hexasaccharide [$\mathbf{I}_{2S}$-$\mathbf{A}^{6S}{}_{NS}$]$_3$. Utilising these four chemically defined oligosaccharides allows the sulfation pattern specificity of the interaction between **OXT** and heparin to be investigated, possibly providing a means of decoupling the anticoagulant properties of heparin from those involved in the interaction with **OXT**.

The backbone of this study involved measuring a series of ^{15}N–^{1}H and ^{13}C–^{1}H HSQC NMR spectra of **OXT** alone and in the presence of the different heparin derivatives at a range of different temperatures. By quantifying the chemical shift (CS) perturbations (ΔCS) we were able to observe the interaction between **OXT** and the polysaccharides, map the binding determinants/epitopes on the molecules and determine binding constants. By perturbing the temperature of the system, we were able to gain further insights into the interaction mechanism.

2. Methods and materials

2.1 Nomenclature

I stands for iduronate, **G** for glucuronic acid, **A** for glucosamine, **ΔU** for an unsaturated uronic acid and nr indicates that the residue is at the nonreducing end of the molecule. The sub- and superscripts denote the position of sulfation (S) or acetylation (NAc), respectively. **AN** and **IN** refer to position N (either C atom or H atom depending on the context) of the glucosamine or iduronate residue, respectively. For example, $\mathbf{I}_{2S}$-$\mathbf{A}^{6S}{}_{NS}$ corresponds to the disaccharide 2-*O* sulfated iduronic acid linked to 6-*O*-sulfated *N*-sulfated glucosamine. **A2*** signifies position 2 of glucosamine, which is *N*-sulfated and *O*-sulfated at positions 6 and 3.

2.2 Reagents

The acetate salt of **OXT** was purchased from Bachem (Bubendorf, Switzerland), with a disulfide bond between Cys1 and Cys6 formed. Sodium fondaparinux ($\mathbf{A}^{6S}{}_{NS}$-$\mathbf{G}_{2OH\text{-}3S}$$\mathbf{A}^{6S}{}_{NS}$-$\mathbf{I}_{2S}$-$\mathbf{A}^{6S}{}_{NS}$-**OMe**) and **DAL** (EDQM CRS) were sourced from Sigma Aldrich, UK. While, the heparin hexasaccharides (**DP6** ([$\mathbf{I}_{2S}$-$\mathbf{A}^{6S}{}_{NS}$]$_3$), **DP6-NAc** ([$\mathbf{I}_{2S}$-$\mathbf{A}^{6S}{}_{NAc}$]$_3$), **DP6-6OH** ([$\mathbf{I}_{2S}$-$\mathbf{A}^{6OH}{}_{NS}$]$_3$) and **DP6-2OH** ([$\mathbf{I}_{2OH}$-$\mathbf{A}^{6S}{}_{NS}$]$_3$)) were purchased from Iduron (Cheshire, UK).

2.3 NMR sample preparation

The **OXT** and **FP** samples used for assignment contained 4 and 2 mM, respectively. Samples used for binding epitope mapping contained 3.3–4 mM **OXT** and 0.9 : 1, 1.7 : 1 and 3.3 : 1 molar ratios of **DP6**/**DP6-NAc**/**DP6-6OH**/**DP6-2OH**, **FP** and **DAL**, respectively. Titration experiments were carried out by step-wise addition of concentrated polysaccharide solution into a 2 mM **OXT** sample (0.14 and 0.2 mM **DAL** and **FP**, respectively). All samples described above were dissolved in 10 mM phosphate buffer, pH 6.0 supplemented with 10% D_2O and 50 μM 4,4-dimethyl-4-silapentane-1-sulfonic acid (DSS). Samples used to investigate the hydroxyl signals contained 2 mM **FP** and 4 mM **OXT** and were made up in 25% d_6-acetone (v/v), pH 8.2 and 0.15 M NaCl. In this buffer system, the samples were still liquid at 285.5 K.[21]

2.4 NMR measurements

All NMR experiments were carried out on a Bruker Avance NEO 700 MHz spectrometer equipped with a QCI-F cryoprobe (Bruker, Coventry, UK). Water suppression was achieved using excitation sculpting with gradients.[22] Phase sensitive 2D-HSQC spectra were acquired using Echo/Antiecho-TPPI gradient selection (Bruker pulse sequences – *hsqcetgpsisp.2* and

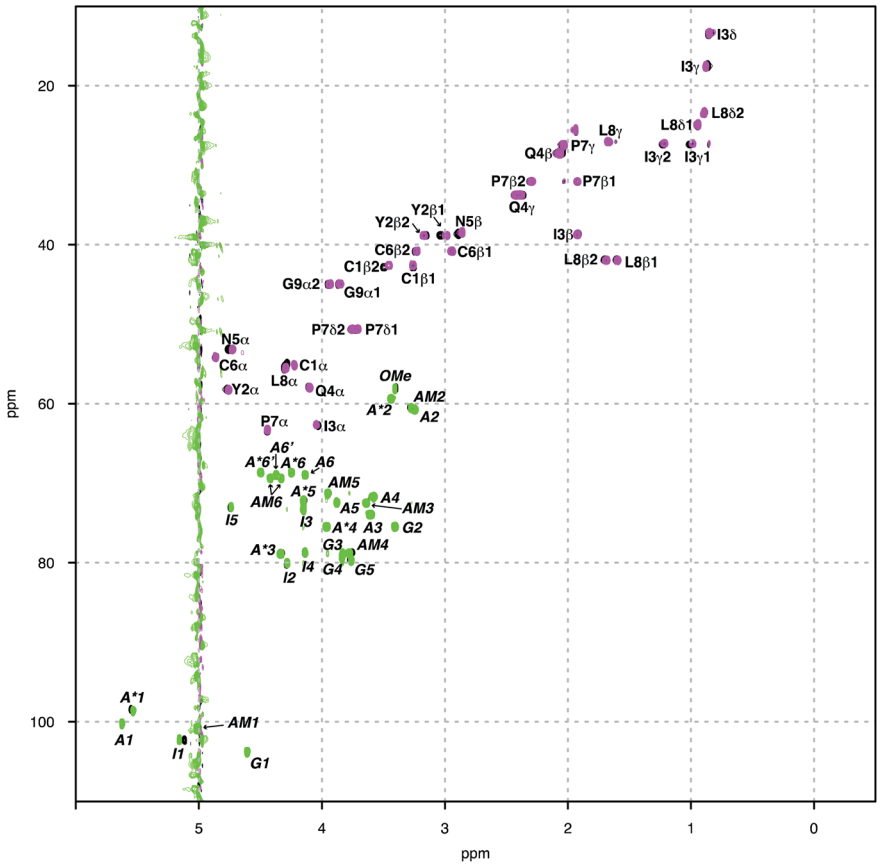

Fig. 2 $^{1}H-^{13}C$-HSQC NMR spectra overlay of **OXT** : **FP** 1.7 : 1 (black), **OXT** only (magenta) and **FP** only (green). $^{1}H-^{13}C$-HSQC NMR Spectra collected at 280 K. Peaks are labelled with assignment in regular and *italic* font for **OXT** and **FP**, respectively. It can clearly be seen by visual inspection that the following signals are perturbated upon interaction; **FP** – G4, A*1, A*3, I1, I2, I4, I5 and A_M4; **OXT** – C1β, Y2α, Y2β, I3α, I3γ12, I3γ13 and I3γ12, N5α, N5β, L8α.

hsqcetfpf3gpsi for ^{13}C and ^{15}N, respectively). Total Correlation Spectroscopy (TOCSY) spectra were acquired using the DIPSY2 sequence, with a mixing time of 80 ms (Bruker pulse sequence – *dipsi2esgpph*), while Nuclear Overhauser Effect Spectroscopy (NOESY) spectra were collected with a mixing time of 200 ms (Bruker pulse sequence – *noesyesgpph*). Typical carrier positions used in all experiments were 117 ppm for ^{15}N, 75 ppm for ^{13}C and 4.7 ppm for ^{1}H. Experiments were carried out at a range of temperatures as noted in the text. Titration experiments were carried out at 280 K and hydroxyl NMR investigation were performed at 258.5 K. Data were processed and analysed using Topspin 4.0.3 (Bruker, Karlsruhe, Germany) software.

2.5 Chemical shifts assignment

The following references were used to assign the molecules investigated in this study: **OXT**,[23] **FP**,[24] **DAL**[15] and **DP6**/**DP6-NAc**/**DP6-6OH**/**DP6-2OH**.[25,26]

2.6 ΔCS perturbations

Chemical shift (CS) perturbations for each atom where simply calculated by subtracting the CS value of the free molecule, $CS^{Free}_{nuclei\ x}$, from that of the bound molecule $CS^{Bound}_{nuclei\ x}$. For example, for ^{1}H:

$$\Delta CS_H = CS_H^{Bound} - CS_H^{Free} \quad (1)$$

The weighted changes in chemical shift are then calculated:

$$\Delta CS_{HN} = \sqrt{(\Delta CS_H)^2 + (\Delta CS_N/10)^2}, \text{ for } {}^{1}H - {}^{15}N \text{ HSQC} \quad (2)$$

and

$$\Delta CS_{HC} = \sqrt{(\Delta CS_H)^2 + (\Delta CS_C/17)^2}, \text{ for } {}^{1}H - {}^{13}C \text{ HSQC}. \quad (3)$$

Residues are considered to be involved in binding if they experience a ΔCS larger than the mean plus one standard deviation for $^{15}N-^{1}H$ chemical shift perturbations and the mean plus three standard deviations for $^{13}C-^{1}H$ chemical shift perturbations.[27,28] The means and standard deviations were determined temperature wise.

2.7 Evaluation of the dissociation constants

The use of chemical shift changes upon binding to evaluate dissociation constants is well established. The complex concentration can be indirectly measured from the weighted changes in chemical shifts (eqn (2)) and their dependence on the concentration of the added polysaccharide. Thus, allowing determination of its dissociation constant. The changes in

chemical shift were plotted as a function of the added peptide concentration and assuming a 1 : 1 simple binding model, K_D = [O][Ps]/[OPs] were fit globally to the equation:

$$\Delta CS/\Delta CS_0 = \left((a+1+x) - \sqrt{(a+1+x)^2 - 4x}\right)\Big/2 \quad (4)$$

where [O] and [Ps] represent the concentrations of **OXT** and the ligand polysaccharides, respectively, x = [Ps]/[O] and ΔCS_0 and $a = K_D$/[O] were fitted by Origin 2019 (Originlab, MA, US). This approach was previously implemented in Schnur *et al.*[29]

3. Results and discussion

Herein we study the interaction between **OXT** and the LMWH **DAL**, as well as the model oligosaccharides, **DP6** and **FP**, that represent sequences found in **DAL**. These interactions were studied by measuring a set of ^{15}N–^{1}H and ^{13}C–^{1}H HSQC NMR spectra of the complexes at different temperatures (280–328 K in 6 K steps). The binding epitopes were mapped by comparing the differences between the chemical shifts of the free and bounds molecules (ΔCS perturbations). If the ΔCS is zero then the chemical environment around the molecule being observed has not changed on the addition of the ligand and no interaction has taken place. Analysis of the ΔCS_{HN} perturbations allowed the peptide to be observed solely, primarily the peptide backbone. While, the ΔCS_{HC} perturbations could be used to observe both the peptide (backbone and side chains) and carbohydrates. The signals were generally well dispersed, with no overlap between the peptide and carbohydrate features (Fig. 2). Dalteparin is a heterogenous mixture of polysaccharide chains of different length and with a variety of sequences. As such, it gives rise to broadened peaks in its NMR spectrum, which are harder to interpret and difficult to assign specifically. However, **FP** and **DP6**, which are shorter, are more amenable to NMR studies (Fig. 1). Thus, allowing us to study the reciprocal

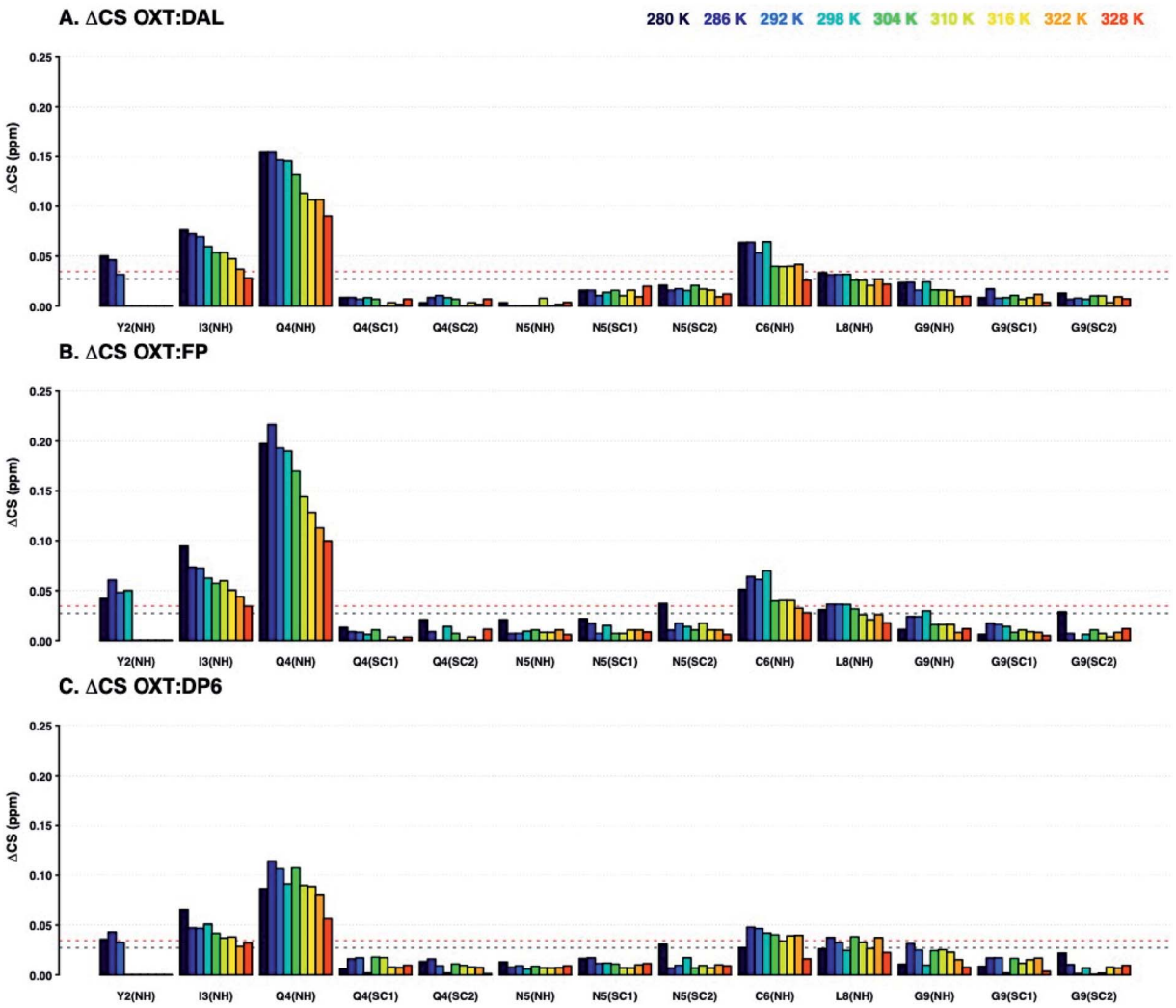

Fig. 3 Change in ^{15}N–^{1}H chemical shifts of residues of OXT upon binding to DAL (A.), FP (B.), or DP6 (C.) at a range of temperatures (280–328 K in 6 K steps, dark blue to red, respectively). The *Y* axis shows ΔCS in ppm (see Materials and methods). The *X* axis indicated the atom in the amino acid, 'SC' stands for side-chain. The figure illustrates that the binding epitope in OXT for heparin-related oligosaccharides involved Y2(NH), I3(NH), Q4, C6(NH) and L8(NH). The horizontal lines indicate ΔCS values larger than the mean (black dotted lined) and larger than the mean plus one standard deviation (red dotted line).

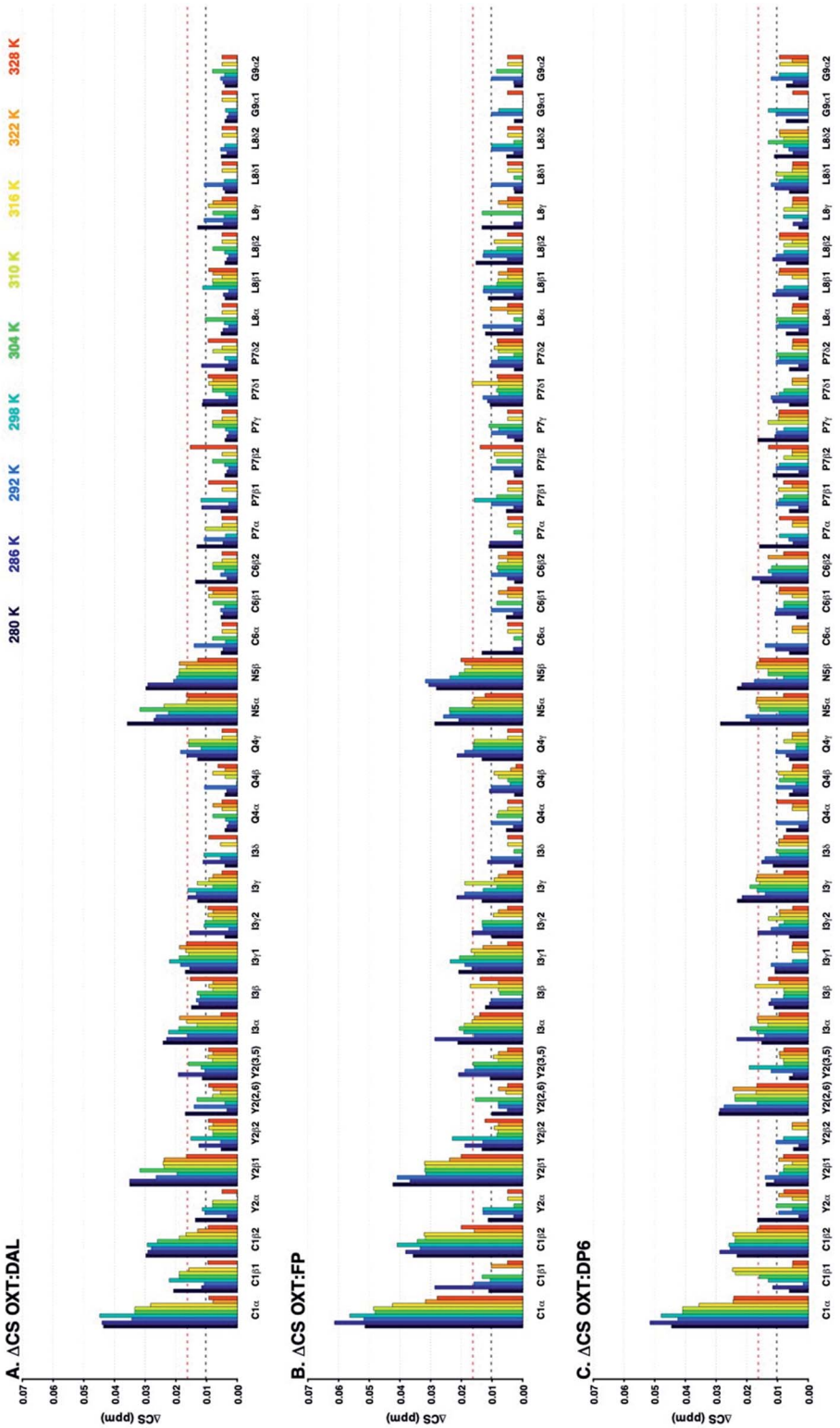

Fig. 4 Changes in the $^{13}C-^{1}H$ chemical shifts of **OXT** residues upon binding to **DAL** (A), **FP** (B) or **DP6** (C) at a range of temperatures (280–328 K in 6 K steps, dark blue to red, respectively). The *Y* axis shows ΔCS in ppm (see Materials and methods) and the *X* axis indicate the atom in the amino acid. The figure indicates that the binding **OXT** interaction epitope for heparin related oligosaccharides involves; **C**1, **Y**2, **I**3, **Q**4 and **N**5. The horizontal lines indicate ΔCS values larger than the mean (black dotted lined) and larger than the mean plus three standard deviations (red dotted line).

effect of **OXT** on **FP** and **DP6.** Furthermore, three chemical modified heparin hexasaccharides (**DP6-NAc**, **DP6-2OH** and **DP6-2OH**) were used, in conjunction with, **DP6** to study the heparin chemical space, investigating whether any particular moiety ($\mathbf{I}_{2S}$, $\mathbf{A}^{6S}$ or $\mathbf{A}_{NS}$) was vital for the interaction between **OXT** and heparin.

3.1 Mapping the binding site of OXT to DAL, FP and DP6

The following molar ratios were used to map the binding site of **OXT** to **DP6**, **FP** and **DAL**; 0.9 : 1, 1.7 : 1 and 3.3 : 1, respectively. The rationale behind these values is related to the heterogeneity of the oligosaccharides and their respective lengths. Dalteparin has an average molecular weight of ~6000 Da, which equates to an approximate length of 18–20 disaccharide units. When compared to **DP6**, which is a hexasaccharide, **DAL** can interact with many peptides given that it is approximately 3 times longer in length. Furthermore, **DAL** and **DP6** are heterogenous, containing a mixture of oligosaccharides with different sulfation patterns and containing chains with the uronic acids in both iduronic and glucuronic acid formed. Unlike, **FP** which is a chemically synthesised pentasaccharide with a defined sequence (**A6S$_{NS}$-G$_{2OH}$-$_{3S}$A$^{6S}_{NS}$-I$_{2S}$-A$^{6S}_{NS}$-OMe**), therefore less of the material is required when compared to **DP6** to obtain a similar response.

Analysis of the chemical shift perturbations in the ^{15}N–^{1}H HSQC NMR spectra (ΔCS_{HN}) shows that the peptide interacts with **DAL**, **FP** and **DP6** in a similar manner. The binding site mainly involves **I**3, **Q**4 and **C**6 and to a lesser extent **Y**2 and **L**8 (back bone amides, Fig. 3). Judging from the ΔCS values of **I**3 and **Q**4, the interaction between **OXT** and both **FP** and **DAL** becomes stronger as the temperature of the complex is decreased, suggesting it is a favourable energetic state. It should be noted that the ^{15}N–^{1}H backbone peak of **Y**2 does not appear and could not be assigned at temperatures higher than 298 or 304 K. This could imply some structural flexibility of **OXT**.

Analysis of the ΔCS_{HC} perturbations suggests that the interaction of **OXT** with the carbohydrate involves residues **Y**2 (β), **I**3 (α and γ) and **Q**4 (not seen in **OXT** : **DP6**) as seen with the ΔCS_{HN} perturbations. Also, **C**1 (α and β) and **N**5 (α and β) participate in binding (Fig. 4). That is, binding of the heparin polysaccharides (**DAL**, **FP** and **DP6**) affects mainly the ring of **OXT** (residues 1–6), rather than its tail (residues 7–9). Interestingly, residues found across the ring are involved, suggesting a "face-on" interaction where the polysaccharides lie across the cyclic nonapeptide ring, a schematic of the affected atoms in **OXT** can be seen in Fig. 11. The first impression from a comparison of the three panels of Fig. 3 and 4, is a striking similarity between the effects of the three heparin derivatives on **OXT**; a not unexpected result, as the three derivatives are closely related and have much in common. However, a couple of slight differences can be found; the side-chain of **Q**4 is less affected in the presence of **DP6** in comparison to **DAL** and **FP**, suggesting, perhaps, an involvement of either the hydroxyl groups of glucuronic acid or the triply-sulfated *N*-glucosamine. Likewise, the effect seen on **C**6 only with **DAL** suggests it is brought about by groups that do not appear on both **FP** and **DP6** or, is due to the long chain oligosaccharides found in **DAL**.

It is worth mentioning that at higher temperatures, the **OXT** spectrum exhibited a population of secondary peaks, that grows

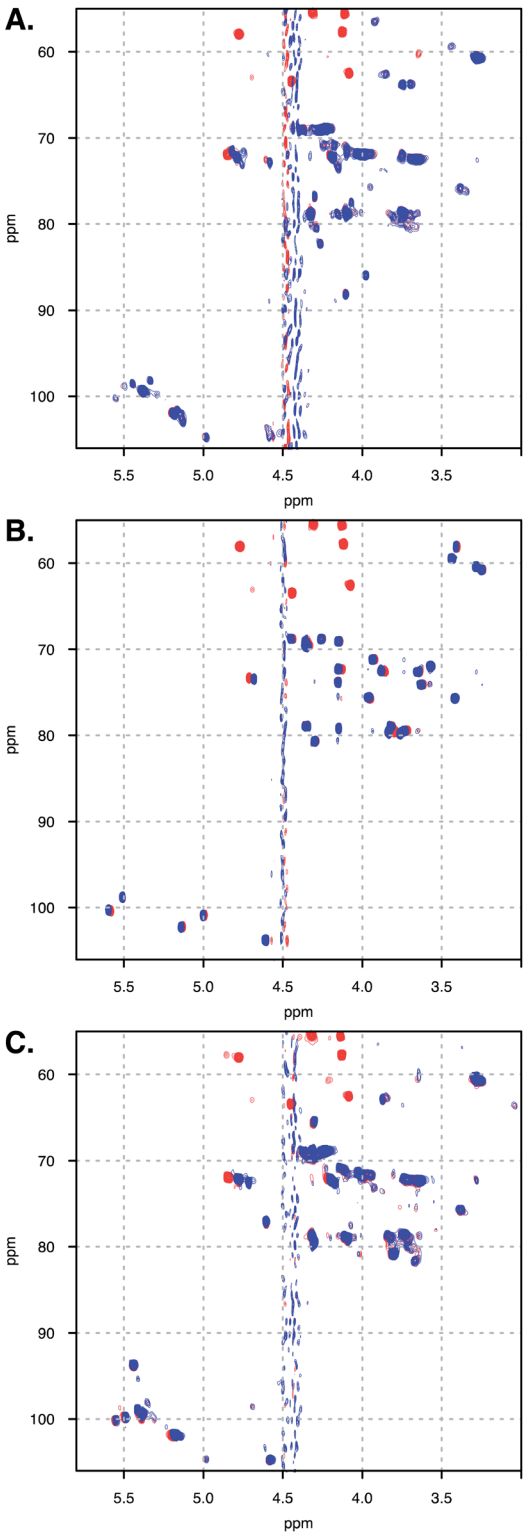

Fig. 5 Spectra overlay of free (A) **DAL**, (B) **FP** and (C) **DP6** (blue), and in complex with **OXT** (red). Spectra measured at 328 K.

stronger with increased temperatures, suggesting, once more that **OXT** can exist in a secondary, less energetically favourable, conformation.

3.2 Mapping the binding site of DAL, FP and DP6 to OXT

In addition to observing the peptide, ΔCS_{HC} perturbations allowed the effects of the interaction on the carbohydrate to be mapped as well. Dalteparin is not best suited for peak assignment and ΔCS_{HC} determination with high confidence as it is a highly heterogenous mixture of polysaccharide chains with different substitutions and lengths (Fig. 1A). Therefore, model compounds approximating regions within **DAL** were studied, **FP** and **DP6** (Fig. 1C and D, respectively).

Owing to its low molecular weight, the NMR spectra of **FP** contain sharp, well defined spectral features that allowed analysis and full assignment (example in Fig. 2 and 5B), enabling the study of the reciprocal effect of **OXT** on **FP**.

The ΔCS_{HC} results for **FP** upon binding **OXT** are presented in Fig. 6A. Atoms on the **G**2, **A***3, **I**4 and $\mathbf{A_M}$5 rings of **FP** (Fig. 1) experience changes in their chemical shifts in the presence of **OXT** (Fig. 6A). The spread of the effect over the length of the polysaccharide agrees with the notion of a "face-on" interaction between the sugar and the ring of **OXT**.

Interestingly, the trend of change with temperature differs for different atoms and two distinct effects can be seen in the **OXT** : **FP** interaction. Firstly, ΔCS_{HC} decreases with increasing temperatures for **I**4–1 and $\mathbf{A_M}$5–4, as seen for **OXT** residues. However, the opposite is seen for position-5 of both the glucuronic and iduronic acid residues. This counter-intuitive behaviour, where ΔCS_{HC} perturbations increase with higher temperatures, could be explained by perturbation of the hydrogen-bonding network formed by these acid groups due to **OXT** binding, whether by **OXT** interacting directly with the carboxylic groups of rings **I**4 and $\mathbf{A_M}$5 (Fig. 1) or by **OXT** imposing a conformational change in the saccharide that does not sustain the otherwise favourable hydrogen bond network. Interestingly, atoms **A***3–1, **I**4–1 and $\mathbf{A_M}$5–4 are involved, suggesting perhaps a change in the glycosidic bonds centred around **I**4. It should be noted that position-5 of the uronic acid residues are very sensitive to their environment.

The heparin-derived hexasaccharide, **DP6**, were produced by depolymerising heparin by using heparinase 1 and then separation by high-resolution gel chromatography, therefore, they are size defined but not sequence defined, containing primarily, but not solely, the trisulfated repeating unit $\mathbf{I_{2S}}$-$\mathbf{A^{6S}_{NS}}$ (Fig. 1D). Hence, it was not surprising that its NMR spectra revealed the presence of structures which were not the majority structure $\mathbf{I_{2S}}$-$\mathbf{A6S_{NS}}$, such as GlcA (Fig. 5C). This is most likely as a result of not being chemically synthesised but rather biologically sourced.

Thus, our sample is a mixture of short polysaccharide chains with a majority of, but not exclusively, the **DP6** structure. As

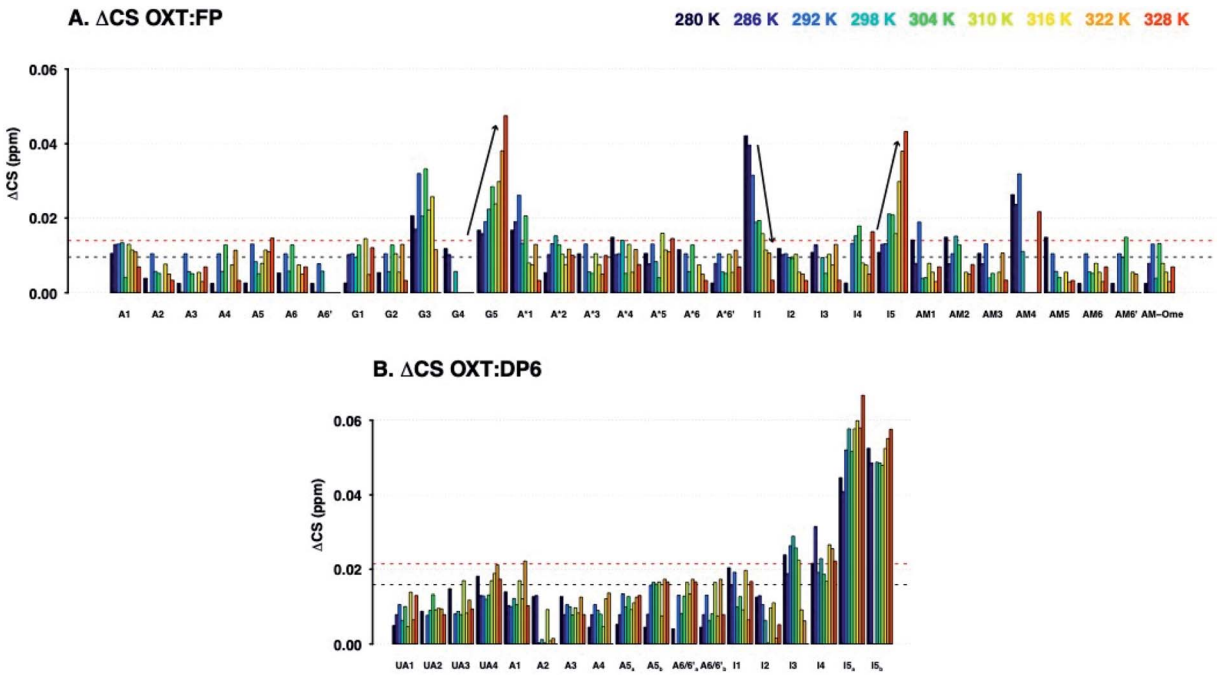

Fig. 6 Change in $^{13}C-^{1}H$ chemical shifts of FP (A) and DP6 (B) residues upon addition of OXT at a range of temperatures (280–328 K in 6 K steps, dark blue to red, respectively). The *Y* axis showing ΔCS in ppm (see Materials and methods) and the *X* axis indicates the residue and atom in the polysaccharide (For DP6 (B) residue numbers not assigned). The horizontal lines indicate ΔCS values larger than the mean (black dotted lined) and larger than the mean plus three standard deviations (red dotted line).There are two different phenomena observed as the temperature increased, firstly the ΔCS for G3, I1, A1* and A_M4 in FP decreases upon the change in temperature, this is similar to what is observed in OXT. Conversely, the ΔCS for G2–5 and I4–5 in FP increases as the temperature is increased, it is hypothesized that is due to changes in the hydrogen bond-network between the carboxyl groups and the surrounding water. This is also observed in the more heterogenous DP6, the ΔCS for I5a and I5b both also increase.

evident from a comparison of panels A and C in Fig. 5, this leads to NMR spectra with a certain level of complexity which prevented sequence specific assignment. We were, however, able to assign families of peaks to atom types (Fig. 6B), allowing us to study the interaction of **DP6** to **OXT** and compare it to the that of **FP**. As with **FP**, the iduronic acid seems to be affected by the presence of **OXT** and specifically atom 5 and to a lesser extent its neighbouring atom 4. Interestingly, peaks assigned to position-3 of glucuronic acid also experienced a change in chemical-shift similar, again, to the observation with **FP** (data not shown). This suggests an important role for glucuronic acid in the interaction with **OXT**.

Unfortunately, the heterogenous nature of **DAL** renders it difficult to analyse by NMR, in which this heterogeneity gives rise to peak broadening. Still, the ^{13}C–^{1}H HSQC NMR spectra of **FP**, **DP6** and **DAL** are closely related, as clearly evident from Fig. 5. When comparing the overlaid spectra of each of the polysaccharides alone and in the presence of **OXT**, a great similarity is revealed. For example, the peaks around 4.8 and 72 ppm, which in **FP** is assigned to **I**5, experience a change in chemical-shift in all cases while peaks around 3.3 and 61 ppm, assigned to **A**2 and $\mathbf{A_M}$2 in **FP**, do not change position in all polysaccharides. Thus, we feel confident that the information learned for **FP** and **DP6** can be used to approximate the interactions of **DAL** with **OXT** as well.

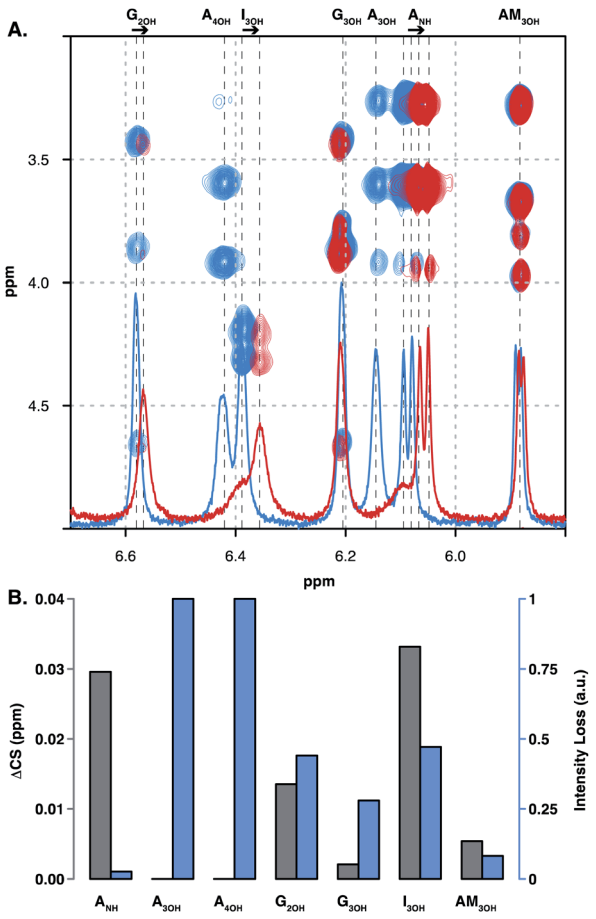

Fig. 7 Low temperature NMR of the carbohydrate amine and hydroxyl groups. (A) Overlay of TOCSY and 1D-^{1}H spectra of **OXT** alone (blue) and in complex with **FP** (red). Assignments of hydroxyl residues of **FP** appear on the bottom. Arrows indicate system shifts. (B) ΔCS of hydroxyl residues of **FP** in the F2 dimension (grey bars) and normalised signal intensity loss (blue bars; 0 = no intensity change and 1 = the signal has completely disappeared).

3.2.1 Sulfates are not the only chemical groups involved in the interaction between OXT and FP. Hydroxyl and amine residues are among the chemically active groups of carbohydrates, which do not appear in a ^{13}C–^{1}H HSQC spectrum and are solvent exchangeable, therefore, not visible under experimental conditions usually employed. However, Beecher *et al.* demonstrated that at low temperatures it is possible to observe the solvent exchangeable hydroxyl and amine protons present in **FP**.[21] Although hydrogen bonds have previously been identified to be import for heparin:protein interactions,[30] they are rarely investigated in solution. One-dimensional ^{1}H and TOCSY NMR spectra of **FP** alone and in the presence of **OXT** at 258.5 K were acquired (dissolved in 25% d_6-acetone (v/v) to prevent sample freezing; Materials and methods). Signals from **A**1–NH, **A**1–OH3, **A**1–OH4, **G**2–OH2, **G**2–OH3, **I**4–OH3 and **A**5–OH3 can be observed for **FP** (Fig. 7). Two phenomena can be observed upon binding of **FP** to **OXT**: change of signal intensity and position. Signals assigned to **A**1–NH and **I**4–OH3 significantly had their CSs perturbated upon binding (Fig. 7). The chemical group **G**2–OH2 also experienced chemical shift changes but to a lesser extent. Features arising from **G**2–OH2, **G**2–OH3 and **I**4–OH3 lost intensities upon binding, while **A**1-OH3 and **A**1–OH4 did not appear in the spectra of the bound oligosaccharide (Fig. 7). The changes in hydroxyl signals in the **FP** spectra upon addition of **OXT**, suggest the interaction affects the hydrogen bond network of **FP** or its structure. The presence of the two phenomena, peak position shift and intensity loss, suggest a complex interaction between **FP** and **OXT** with different processes occurring on different time scales.

3.2.2 The effect of heparin substitution pattern on the interaction. To further investigate the interaction between heparin and **OXT** three chemically modified hexasaccharides were sourced (**DP6-NAc**, **DP6-6OH** and **DP6-2OH**), allowing the chemical space of heparin to be investigated. In these experiments the concentration ratio of **OXT** and the 4 ligands is the same, therefore the magnitude of the ΔCS can be compared directly. When using the 3 chemically-modified hexasaccharides it is noticeable that the unmodified hexasaccharide ($[\mathbf{I_{2S}}\text{-}\mathbf{A}^{6S}{}_{NS}]_3$) causes the greatest change in ^{15}N–^{1}H chemical shift perturbations (Fig. 8), indicating that the interaction between the peptide and **DP6** is the strongest and that there is a charge component to the interaction, which is not unexpected. The ^{15}N–^{1}H chemical shift perturbation profiles for **OXT : DP6-6OH**, **OXT : DP6-2OH** and **OXT : DP6-NAc** are very similar, with the ΔCS for **OXT : DP6-NAc** being attenuated. The primary difference is seen at **I**3-NH and **Q**4-NH, suggesting that the hexasaccharide is interacting with these amino acids *via* the *N*-sulfate, located at position-2 of glucosamine.

The ^{13}C–^{1}H chemical shift perturbation profiles are different between **DP6** and the chemically-modified hexasaccharides (Fig. 9). Firstly, the fully sulfated hexasaccharide, **DP6**, affects the ring of the tyrosine residue at position-2 more than the

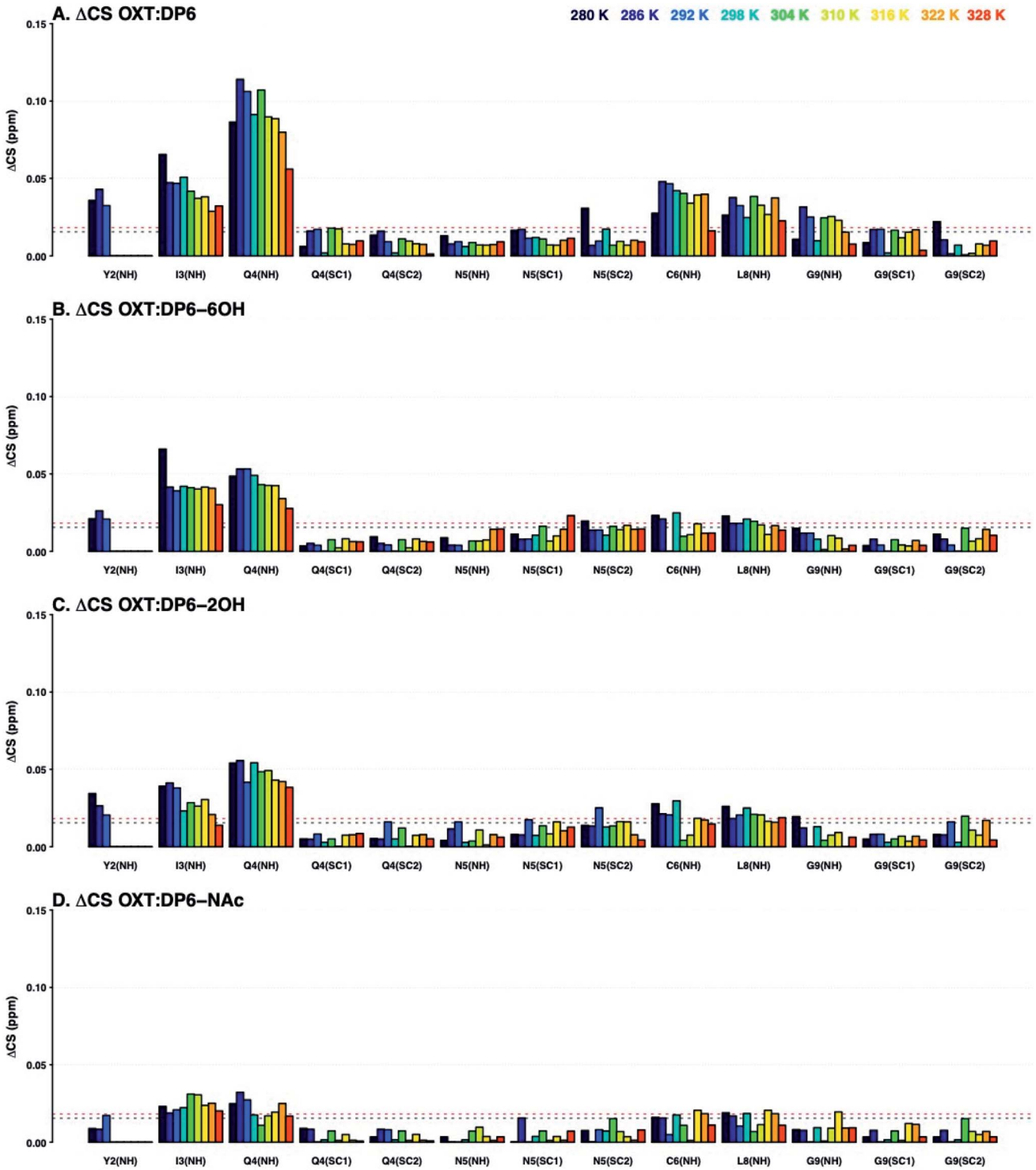

Fig. 8 Change in $^{15}N-^{1}H$ chemical shifts of residues of **OXT** upon binding to **DP6** (A), **DP6-6OH** (B), **DP6-2OH** (C) or **DP6-NAc** (D) at a range of temperatures (280–328 K in 6 K steps, dark blue to red, respectively). The *Y* axis shows ΔCS in ppm (see Materials and methods). The *X* axis indicates the atom in the amino acid, 'SC' stands for side-chain. The ΔCS are attenuated in the **OXT** : **DP6-NAc** complex (I3(NH) and Q4(NH)), indicating that *N*-sulfation of the glucosmine is important for the interaction with the peptide. The horizontal lines indicate ΔCS values larger than the mean (black dotted lined) and larger than the mean plus one standard deviation (red dotted line).

chemically modified hexasaccharides. Secondly, in the interaction with the peptide's *N*-terminal residue, **C1**, the effect seen with **DP6** is inverse to that observed in the presence of **DP6-NAc**, **DP6-2OH** or **DP6-6OH**. The inverse temperature effect indicates that as the temperature increases, the chemical environment experienced by **OXT** in the complex become more similar to that of **OXT** alone. Whereas, the effect of the interaction between **DP2-2OH** [$\mathbf{I_{2OH}}$-$\mathbf{A^{6S}_{NS}}$] and **DP2-NAc** [$\mathbf{I_{2S}}$-$\mathbf{A^{6S}_{NAc}}$] and **OXT**

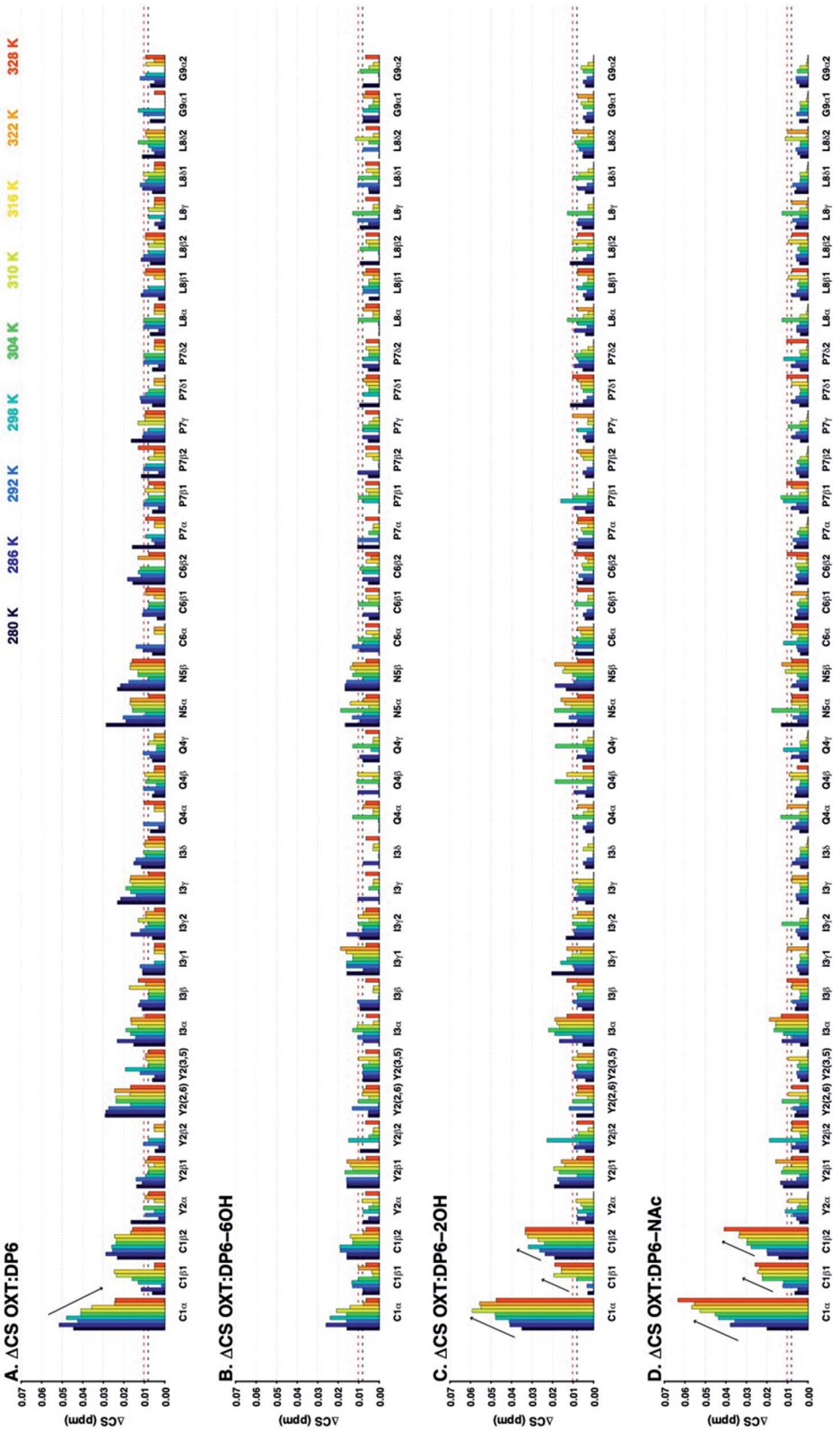

Fig. 9 Change in $^{13}C-^{1}H$ chemical shifts of residues of **OXT** residues upon binding to **DP6** (A), **DP6-6OH** (B), **DP6-2OH** (C) or **DP6-NAc** (D) at a range of temperatures (280–328 K in 6 K steps, dark blue to red, respectively). The *Y* axis shows ΔCS in ppm (see Materials and methods). The *X* axis indicates the atom in the amino acid. The ΔCS are attenuated in the **OXT** : **DP6-6OH** complex (**C1**), indicating that 6-*O*-sulfation of the glucosamine is important for the interaction with the peptide. In addition there is an inverse temperature effect observed at the N-terminus amino acids of the peptide for the **OXT** : **DP6** complex (see arrows), which is not observed in the interactions between **OXT** and **DP6-NAc**, **DP6-2OH** or **DP6-6OH**. The horizontal lines indicate ΔCS values larger than the mean (black dotted lined) and larger than the mean plus three standard deviations (red dotted line).

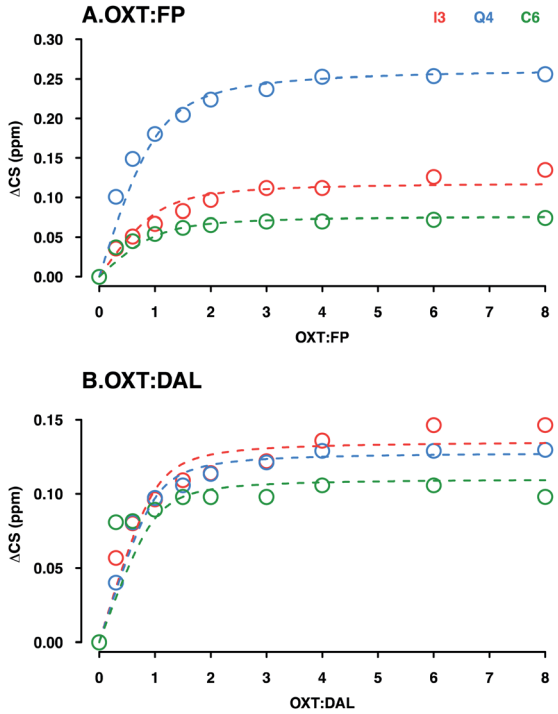

Fig. 10 Determination of the K_D for the interaction between OXT : FP (A) and DAL (B). Plots illustrate the ΔCS of OXT residues (I3, Q4 and C6 in red, blue and green, respectively) as a function of carbohydrate concentration. Oxytocin was titrated with either FP (A) or DAL (B). The weighted changes in chemical shifts (ΔCS) in the $^{15}N–^{1}H$ HSQC spectra were calculated using eqn (2) (Materials and methods). The curves were fit globally to ΔCS as a function of added concentration according to eqn (3) (Material and methods) using the OriginLab software.

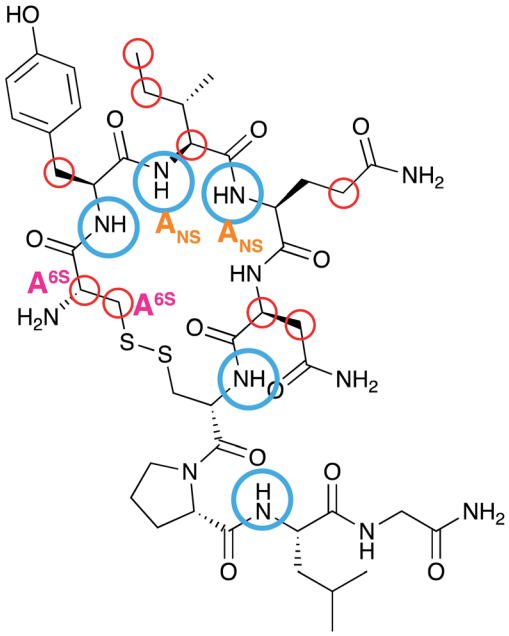

Fig. 11 A schematic highlighting the collated atoms within OXT that were identified to interact with heparin. The atoms highlighted in blue were identified in the $^{15}N–^{1}H$ ΔCS experiments and the red identified in the $^{13}C–^{1}H$ ΔCS measurements. The schematic indicates the atoms that were affected by specific substituent groups of heparin. The N-terminus residue C1, was affected by de-6-*O*-sulation (magenta) of the heparin hexasaccharide. While the amines of I3 and Q4 were affected by de-*N*-sulfation (orange) of the heparin hexasaccharide. The depiction above illustrates that the interaction with heparin occurs across the face of the cyclic nonapeptide, with even the smallest oligosaccharide, FP, being able to interact with the entire length of oxytocin.

increases as the temperature increases. Sulfation at position-6 of glucosamine is important for the interaction between **OXT** and the heparin hexasaccharides, **DP6-NAc** and **DP6-2OH** greatly perturb the cysteine amino acid, which this is not seen in the **OXT : DP6-6OH** complex, as the 6-*O*-sulfate group is not present to interact with the N-terminus of the peptide. This effect is more specific than simple electrostatic forces causing the chemical-shift perturbations, as **DP6-6OH** and **DP6-2OH** have the same overall charge. Also, the effect **DP6** has on **Y**2 and **I**3 is interesting, as neither of these amino acids is charged, and **DP6** is the most charged of the heparin hexasaccharides.

The combination of measuring $^{15}N–^{1}H$ and $^{13}C–^{1}H$ chemical shift perturbations while the **OXT**:hexasaccharide complexes undergo a thermal gradient illustrates that all four hexasaccharides interact with **OXT**. It was observed that *N*-sulfation and 6-*O*-sulfation of glucosamine are important for the interaction between heparin and **OXT**. Removing the *N*-sulfate group and replacing it with an *N*-acetyl moiety attenuated the ΔCS at **I**3 and **Q**4 (Fig. 8), while de-6-*O*-sulfation diminished the ΔCS of **C**1 (Fig. 9). These two sulfate groups have two different effects on the polysaccharide chain. 6-*O*-Sulfation is a charge in space and de-6-*O*-sulfation causes only a local effect. This is not the case for *N*-sulfation, replacing the *N*-sulfate with an *N*-acetly group affects the adjacent linkage, as well as, the conformation of the neighbouring uronic acid residue.[26,31,32]

3.3 Binding constant determination

The binding constant (K_D) was determined by analysing $^{15}H–^{1}H$ HSQC titration experiments where either **DAL** or **FP** were added in a step-wise manner to a sample of **OXT**. Titration experiments were carried out at 280 K, where the interaction is at its tightest and the changes in chemical shift are largest, thus providing more accurate analysis of results.

3.3.1 Three OXT residues. I3, **Q**4 and **C**6 which exhibited the biggest changes in chemical shift upon binding both **DAL** and **FP**, were chosen for the analysis. The weighted changes in chemical shifts (ΔCS_{HN}) between free and bound **OXT** at each addition point were calculated using eqn (2) (Materials and methods) and plotted as a function of carbohydrate concentration (Fig. 10). The curves were fit globally to eqn (4) (Materials and methods). The fitted binding constants are $K_d = 0.33 \pm 0.01$ mM for the interaction between **OXT** and **FP** and $K_d = 0.15 \pm 0.01$ mM for the interaction between **OXT** and **DAL**. That is, the strength of interaction between **OXT** and **DAL** is of the same order of magnitude as the interaction between **OXT** and **FP**.

As **DAL** contains the **FP** sequence, it is perhaps to be expected that the strength of interaction is on the same scale. On the other hand, **DAL** is a heterogeneous mixture of chains with an average length 4 times that of **FP** (**FP** is a penta-saccharide while

the average chain length of **DAL** is 19 saccharides, sufficient to interact with several **OXT** molecules), which might lead to the expectation of tighter interaction with **DAL** as a result of more interacting regions being available. In the case of the **OXT** interaction, however, such reasoning might become nullified as **OXT** itself is very small and of comparable size to the 5-ring polysaccharide **FP**. If the interaction of **OXT** with a pentasaccharide saturates **OXT**, then elongation of the polysaccharide chain will not have the same effect on interaction strength as can be estimated purely by reasoning a larger number of interacting moieties or a larger interaction face.

4. Conclusions

The data shown here illustrate that **OXT**, a cyclic nonapeptide that is used to induce uterine contractions, interacts with the LMWH **DAL** and a series of oligosaccharides; **FP** and **DP6** that mimic the major components found in **DAL**. This is an important observation as it has previously been shown that when **OXT** is administered to a patient that has previously been infused with **DAL**, the time taken for child birth is reduced.[13] This is the first time that this interaction has been studied by NMR spectroscopy.

Using a combination of ^{13}C–^{1}H and ^{15}N–^{1}H HSQC NMR experiments, while subjecting the complex to a temperature gradient, allowed the residues in **OXT** that interacted with the oligosaccharides to be identified. Using ^{15}N–^{1}H HSQC NMR experiments **Y**2, **I**3, **Q**4, **C**6 and **L**8 were identified (Fig. 3 and 8) and the ^{13}C–^{1}H HSQC NMR experiments further identified **C**1 and **N**5 as taking part in the interaction (Fig. 4 and 9). A schematic of the binding epitope of **OXT** can be found in Fig. 11, with the carbohydrates interacting with the peptide across the face of the cyclic ring. These perturbations were observed for the shortest oligosaccharide investigated, the **FP**, indicating that the pentasaccharide can interact with the entirety of the peptide.

To investigate whether one specific substituent was important for the interaction between heparin and **OXT**, a series of hexasaccharides were investigated; the aforementioned **DP6** with 3 chemically-modified hexasaccharides, **DP6-2OH**, **DP6-6OH** and **DP6-NAc**. The de-sulfation affected the interaction of all three chemically derived hexasaccharides, with **DP6-NAc** and **DP6-6OH** having the greatest effect, indicating that 6-*O*-sulfation and *N*-sulfation of glucosamine is important for the interaction between **OXT** and heparin. This is an interesting observation as de-*N*-sulfation and then *N*-acetylation is one mechanism for decreasing the anticoagulation activity of heparin.[33] This strategy concentrates on the sulfate driven interactions between heparin and peptides/proteins and the conformational consequences of de-sulfating the carbohydrate.

Here we also investigated the interaction between **OXT** and **FP** using lower-temperature NMR experiments (258.5 K), allowing hydroxyl and amine groups to be observed. A number of these signals changed in position and/or intensity on interaction with **OXT**, highlighting that in addition to the sulfates, the hydroxyl and amine residues are vital components in the interaction with proteins and peptides. Furthermore, the acid groups of glucuronic and iduronic acid were observed to be perturbed on interaction with **OXT**, this was observed in **DAL**, **DP6** and **FP**. In the chemically defined **FP**, the acid moieties were observed to have a positive ΔCS as the temperature increases, it is hypothesised here that this counterintuitive behaviour could be explained by a strong hydrogen-bond network, which is perturbed as the temperature is changed. These observations illustrate the multi-faceted nature of the interaction between heparin-based oligosaccharides and **OXT**.

Conflicts of interest

There are no conflicts to declare.

Notes and references

1 T. W. Barrowcliffe, *Handb. Exp. Pharmacol.*, 2012, 3–22, DOI: 10.1007/978-3-642-23056-1_1.
2 B. Mulloy, J. Hogwood, E. Gray, R. Lever and C. P. Page, *Pharmacol. Rev.*, 2016, **68**, 76–141.
3 J. Y. van der Meer, E. Kellenbach and L. J. van den Bos, *Molecules*, 2017, **22**, 1025.
4 D. L. Rabenstein, *Nat. Prod. Rep.*, 2002, **19**, 312–331.
5 U. Lindahl, G. Backstrom, M. Hook, L. Thunberg, L. A. Fransson and A. Linker, *Proc. Natl. Acad. Sci. U. S. A.*, 1979, **76**, 3198–3202.
6 E. Gray, B. Mulloy and T. W. Barrowcliffe, *Thromb. Haemostasis*, 2008, **99**, 807–818.
7 J. Amiral, F. Bridey, M. Wolf, C. Boyer-Neumann, E. Fressinaud, A. M. Vissac, E. Peynaud-Debayle, M. Dreyfus and D. Meyer, *Thromb. Haemostasis*, 1995, **73**, 21–28.
8 H. J. Lee, A. H. Macbeth, J. H. Pagani and W. S. Young III, *Prog. Neurobiol.*, 2009, **88**, 127–151.
9 H. H. Dale, *J. Physiol.*, 1906, **34**, 163–206.
10 E. J. Hayes and L. Weinstein, *Am. J. Obstet. Gynecol.*, 2008, **198**, 622.e1–622.e7.
11 F. A. Antoni and S. E. Chadio, *Biochem. J.*, 1989, **257**, 611–614.
12 G. Gimpl, J. Reitz, S. Brauer and C. Trossen, *Prog. Brain Res.*, 2008, **170**, 193–204.
13 G. Ekman-Ordeberg, M. Hellgren, A. Akerud, E. Andersson, A. Dubicke, M. Sennstrom, B. Bystrom, G. Tzortzatos, M. F. Gomez, M. Edlund, U. Lindahl and A. Malmstrom, *Acta Obstet. Gynecol. Scand.*, 2009, **88**, 984–989.
14 U. Lindahl and L. Kjellen, *J. Intern. Med.*, 2013, **273**, 555–571.
15 A. Bisio, E. Urso, M. Guerrini, P. de Wit, G. Torri and A. Naggi, *Molecules*, 2017, **22**, 1051.
16 M. Guerrini, S. Guglieri, A. Naggi, R. Sasisekharan and G. Torri, *Semin. Thromb. Hemost.*, 2007, **33**, 478–487.
17 L. D. Wikingsson and G. Ekman-Ordeberg, *Effect of Tafoxiparin on Cervical Ripening and Induction of Labor in Term Pregnant Women With an Unripe Cervix*, https://clinicaltrials.gov/ct2/show/NCT04000438, accessed 21st April, 2020.

18 B. Casu, P. Oreste, G. Torri, G. Zoppetti, J. Choay, J. C. Lormeau, M. Petitou and P. Sinay, *Biochem. J.*, 1981, **197**, 599–609.
19 J. Choay, M. Petitou, J. C. Lormeau, P. Sinay, B. Casu and G. Gatti, *Biochem. Biophys. Res. Commun.*, 1983, **116**, 492–499.
20 M. Petitou, P. Duchaussoy, I. Lederman, J. Choay, P. Sinay, J. C. Jacquinet and G. Torri, *Carbohydr. Res.*, 1986, **147**, 221–236.
21 C. N. Beecher, R. P. Young, D. J. Langeslay, L. J. Mueller and C. K. Larive, *J. Phys. Chem. B*, 2014, **118**, 482–491.
22 T. L. Hwang and A. J. Shaka, *J. Magn. Reson., Ser. A*, 1995, **112**, 275–279.
23 A. Ohno, N. Kawasaki, K. Fukuhara, H. Okuda and T. Yamaguchi, *Magn. Reson. Chem.*, 2010, **48**, 168–172.
24 M. Hricovini and G. Torri, *Carbohydr. Res.*, 1995, **268**, 159–175.
25 A. Pervin, C. Gallo, K. A. Jandik, X. J. Han and R. J. Linhardt, *Glycobiology*, 1995, **5**, 83–95.
26 E. A. Yates, F. Santini, M. Guerrini, A. Naggi, G. Torri and B. Casu, *Carbohydr. Res.*, 1996, **294**, 15–27.
27 M. P. Williamson, *Prog. Nucl. Magn. Reson. Spectrosc.*, 2013, **73**, 1–16.
28 M. P. Williamson, in *Modern Magnetic Resonance*, ed. G. A. Webb, Springer International Publishing, Cham, 2018, pp. 995–1012, DOI: 10.1007/978-3-319-28388-3_76.
29 E. Schnur, N. Kessler, Y. Zherdev, E. Noah, T. Scherf, F. X. Ding, S. Rabinovich, B. Arshava, V. Kurbatska, A. Leonciks, A. Tsimanis, O. Rosen, F. Naider and J. Anglister, *FEBS J.*, 2013, **280**, 2068–2084.
30 D. Xu and J. D. Esko, *Annu. Rev. Biochem.*, 2014, **83**, 129–157.
31 T. R. Rudd and E. A. Yates, *Mol. Biosyst.*, 2010, **6**, 902–908.
32 E. A. Yates, F. Santini, B. De Cristofano, N. Payre, C. Cosentino, M. Guerrini, A. Naggi, G. Torri and M. Hricovini, *Carbohydr. Res.*, 2000, **329**, 239–247.
33 S. J. Patey, E. A. Edwards, E. A. Yates and J. E. Turnbull, *J. Med. Chem.*, 2006, **49**, 6129–6132.